UDC 621.311.68
https://doi.org/10.32362/2500-316X-2022-10-5-60-72

RESEARCH ARTICLE

Development and research of uninterruptible power supply system for networks with supply voltage up to 24 V

Igor M. Sharov [@], Oleg A. Demin, Alexander A. Sudakov, Alexey D. Yarlykov

MIREA – Russian Technological University, Moscow, 119454 Russia
[@] Corresponding author, e-mail: ctosworld@gmail.com

Abstract

Objectives. Due to the continuous rapid development of renewable energy sources, requirements for secondary power supply systems keep increasing from year to year. Productive uptime for end users is dependent on the efficiency and stability of the power supply system. Such systems should be able to distribute and store energy from renewable sources having various parameters and configurations. Therefore, the present work is aimed at developing technical solutions for efficient uninterruptible secondary power supply systems in low voltage DC networks.

Methods. Advanced circuitry solutions are used for performing pulse conversions with high efficiency. The flexible hardware-software system is used for implementing the parameter control system.

Results. An uninterruptible power supply for low-voltage DC networks is developed. The description of subsystems and calculations for all main elements including the power ones are given. Using a contemporary component base, the system prototype is assembled, configured, and measured by parameters. The presented solutions allow achieving the universality of the system in terms of the input and output voltage range. Support for the fast-charging Power Delivery protocol is integrated. As well as regulating the battery charging current and voltage, the Li+ battery charging controller permits changes in the number of chargeable cells. The monitoring and control unit monitors network parameters and controls the system automation. Using a microcontroller as the control device, it is possible to easily change control parameters by changing software settings. Dual redundancy of the module monitoring the built-in battery parameters is used to ensure the reliability and safety of system functioning. Support for the standardized I^2C communication protocol with a separate power bus allows any necessary sensors to be connected for monitoring system parameters. External high-power devices controlled by a PWM signal may be added, if required. In the paper, the Li+ battery charging profile recommended by the manufacturer is provided.

Conclusions. The designed system provides stable power supply to end users at a power consumption up to 40 W for at least 45 min. The automation demonstrates reliable operation.

Keywords: uninterruptible power supply, control unit, charge controller, Power Delivery standard, charging curve, battery protection system, DC-DC converter, battery balancing

• **Submitted:** 09.11.2021 • **Revised:** 01.07.2022 • **Accepted:** 26.08.2022

For citation: Sharov I.M., Demin O.A., Sudakov A.A., Yarlykov A.D. Development and research of uninterruptible power supply system for networks with supply voltage up to 24 V. *Russ. Technol. J.* 2022;10(5):60–72. https://doi.org/10.32362/2500-316X-2022-10-5-60-72

Financial disclosure: The authors have no a financial or property interest in any material or method mentioned.

The authors declare no conflicts of interest.

НАУЧНАЯ СТАТЬЯ

Разработка и исследование системы бесперебойного питания в сетях с напряжением до 24 В

И.М. Шаров [@], О.А. Демин, А.А. Судаков, А.Д. Ярлыков

МИРЭА – Российский технологический университет, Москва, 119454 Россия
[@] Автор для переписки, e-mail: ctosworld@gmail.com

Резюме

Цели. От эффективности и стабильности систем электропитания зависит время бесперебойной работы конечных потребителей. Такие системы должны иметь возможность распределения и накопления энергии от возобновляемых источников с различными параметрами и конфигурациями. Развитие источников возобновляемой энергии постоянно увеличивает требования к системам вторичного электропитания. Целями работы являются разработка научно-обоснованных технических решений и создание эффективной системы бесперебойного вторичного питания в низковольтных сетях постоянного тока.

Методы. Использованы современные схемотехнические решения для выполнения импульсных преобразований с высокой эффективностью. Для реализации системы контроля параметров применен гибкий программно-аппаратный комплекс.

Результаты. Разработана система бесперебойного питания для низковольтных сетей постоянного тока. Приведено описание работы блоков системы и расчеты основных элементов, в т.ч. и силовых. С применением современной элементной базы собран прототип системы, проведена настройка и измерение ее параметров. За счет представленных решений достигается универсальность комплекса по диапазону входных и выходных напряжений. Интегрирована поддержка современного протокола быстрой зарядки Power Delivery. Примененный контроллер зарядки Li+ аккумуляторов позволяет изменять количество заряжаемых ячеек и регулировать токи и напряжения заряда аккумуляторной батареи (АКБ). Блок мониторинга и управления отслеживает текущие параметры сети и управляет автоматикой системы. Использование микроконтроллера в качестве управляющего устройства дает возможность изменения параметров управления без конструктивных изменений благодаря редактированию программного обеспечения. Для безопасности функционирования системы применено двукратное резервирование модуля контроля параметров встроенной аккумуляторной батареи. Поддержка стандартизированного протокола обмена данными по шине I^2C с отдельной шиной питания позволяет подключать любые необходимые датчики для отслеживания параметров системы. При необходимости могут быть добавлены сторонние устройства повышенной мощности, управляемые сигналом широтно-импульсной модуляции (ШИМ). Приведен рекомендуемый производителями профиль заряда Li+ АКБ.

Выводы. Спроектированная система позволяет обеспечивать стабильное электропитание потребителей с энергопотреблением до 40 Вт в течение времени не менее 45 мин. Автоматика демонстрирует безотказное функционирование.

Ключевые слова: система бесперебойного питания, блок управления, контроллер заряда, протокол Power Delivery, профиль заряда, блок защиты, DC-DC преобразователь, модуль балансировки

• **Поступила:** 09.11.2021 • **Доработана:** 01.07.2022 • **Принята к опубликованию:** 26.08.2022

Для цитирования: Шаров И.М., Демин О.А., Судаков А.А., Ярлыков А.Д. Разработка и исследование системы бесперебойного питания в сетях с напряжением до 24 В. *Russ. Technol. J.* 2022;10(5):60–72. https://doi.org/10.32362/2500-316X-2022-10-5-60-72

Прозрачность финансовой деятельности: Авторы не имеют финансовой заинтересованности в представленных материалах или методах.

Авторы заявляют об отсутствии конфликта интересов.

INTRODUCTION

Due to the development of renewable energy sources including their increased capacity, solutions are required for a number of problems associated with the conversion and storage of energy [1]. Automation systems used for these purposes should be developed using new circuit solutions aimed, among other things, at increasing operating efficiency, speed, and autonomy, at the same time as reducing heat generation, safely preventing abnormal operation, maintaining cost-effectiveness, etc. The standard output voltage of power systems in industrial automation and motor vehicles is 24 V. Such power systems can provide power to low-power devices in case of emergency.

Laying networks for emergency equipment is combined with additional time and material costs. This is especially true for emergency lighting systems in remote locations [2]. Such costs can be reduced by using a separate power supply units in the fixed version as a voltage source. Since the power consumption for sensor operation is low, the operating time of such units is satisfactory in the absence of recharging.

24 V power networks are also used in the security and fire safety systems [3]. In this setting, it is obvious that fail-safe power supply is required even under conditions of network failure. The Shtyl[1] and Bastion[2] companies produce uninterruptible power supplies (UPS) in the form of wall mount boxes. A 24 V power supply is also typically used by audio systems, for example, by a great number of device components manufactured by the MONACOR International company[3, 4]. Here, UPS systems can be integrated into devices in the form of modules or to ensure network continuity as a separate unit. It is also theoretically possible to use 24 V UPS systems to ensure the safety of trucks in the event of grid network failure[5]. UPS systems in the form of separate units are necessary attributes of equipment cabinets. Such systems must ensure safe and stable operation throughout their lifetime.

1. UPS SYSTEM

A conventional UPS system consists of two independent devices capable of operating both independently and together, thus expanding the possibilities of applying and reconfiguring the final product. The structural diagram of the UPS system is shown in Fig. 1.

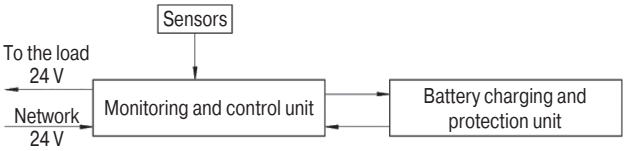

Fig. 1. Structural diagram of the UPS system

The UPS system consists of the monitoring and control unit, battery charging and protection unit, and external sensors. A similar system has been implemented in [4] but using a 220 V power supply.

The monitoring and control unit is designed for controlling the network and battery parameters, as well as the equipment temperature. At the moment of emergency shutdown, the unit commutates the system so that the necessary voltage is supplied from the battery charging and protection unit to the load. This provides the uninterrupted power supply of connected devices from the backup power supply. In addition, output currents and power are monitored while operating from the UPS system. Should the UPS permissible power consumption be exceeded, the load connected to the system is automatically switched off.

The battery charging and protection unit is designed for charging the built-in batteries and equalizing the potential between cells. When the built-in lithium-ion battery is discharged, backup power from any battery having voltage greater than 9 V—e.g., from widespread automotive lead-acid batteries—may be supplied. It is also possible to supply backup power from portable batteries supporting the Power Delivery fast-charging protocol. The unit duplicates critical system protection functions, preventing

[1] https://www.shtyl.ru/. Accessed August 29, 2022 (in Russ.).
[2] https://bast.ru/. Accessed August 29, 2022 (in Russ.).
[3] https://www.monacor.com/. Accessed August 29, 2022.
[4] MONACOR INTERNATIONAL GmbH & Co. KG; 2016. 164 p. https://www.blej24.com/catalogs/Monacor.pdf. Accessed August 29, 2022.
[5] *MAN TGA s 2000 g. Rukovodstvo po remontu i ekspluatatsii* (*MAN TGA from 2000 y. Repair and operation manual*). Monolit; 2015. 794 p. https://monolith.in.ua/catalog/rukovodstvo_po_remontu_man_tga_2000. Accessed August 29, 2022 (in Russ.).

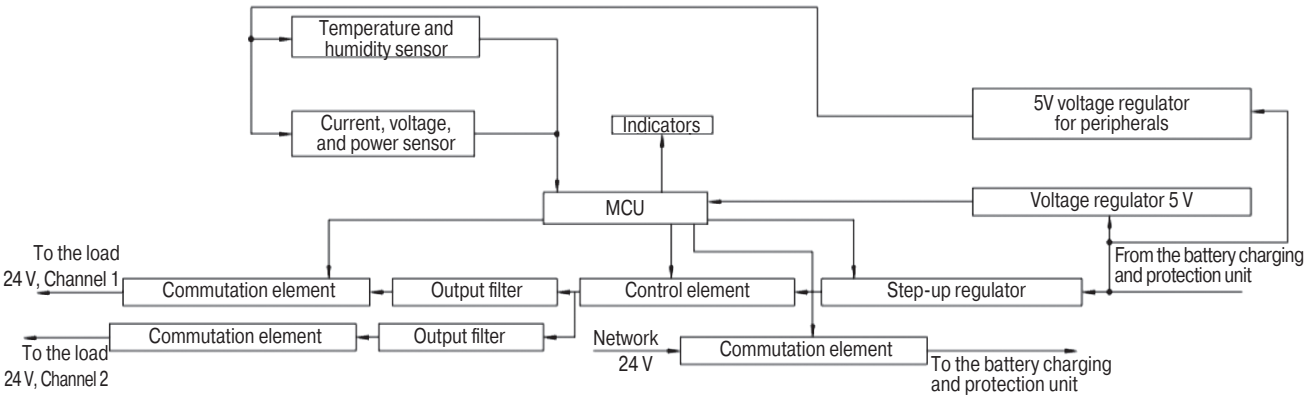

Fig. 2. Structural diagram of the monitoring and control unit

"overcharging" and deep discharging of the battery, as well as monitoring the temperature of the built-in battery using a thermistor.

2. MONITORING AND CONTROL UNIT

In the paper, the monitoring and control unit implemented on the ATmega 168 (Atmel Corporation (Microchip), USA) microcontroller (MCU) is considered [5]. Here, MCU with a clock frequency of 16 MHz, supply voltage, and logic levels of 5 V is used[6]. This version is selected due to its low cost and availability, an especially important factor under the present situation of crisis in the semiconductor industry. If necessary, it can be replaced without serious labor costs by a more productive and energy-efficient unit involving minor modifications of the circuit diagram. The structural diagram of the monitoring and control unit is shown in Fig. 2.

The circuit diagram of the monitoring and control unit shown in Figs. 3, 5, and 6 comprises two 5 V linear voltage regulators, MCU, state indicators, step-up (boost) regulator, three commutation elements, output filters, control element, and connector X1 for connecting sensors via I^2C bus with power supply.

The step-up regulator U1 (Fig. 3) is implemented on an XL6009 chip (XLSEMI, China). With an input voltage ranging from 5 V to U_{out}, its conversion efficiency may achieve 94% depending on the difference between input and output voltages. The conversion frequency is 400 kHz, while the maximum commutated current is 4 A. Soft start, thermal protection, and current limitation functions are built in[7]. The output voltage may be calculated by the following formula:

$$U_{out} = 1.25\left(1+\frac{R_{13}}{R_{14}}\right) = 1.25\left(1+\frac{18\ \text{k}\Omega}{1\ \text{k}\Omega}\right) = 23.75\ \text{V}. \quad (1)$$

Inductances L3 and L4 are switched in parallel for providing a given maximum conversion current. The converter chip has the control input for switching it on connected to the MCU pin via current limiting resistor R11. Resistor R12 connects the MCU pin of the microcircuit to "ground" for preventing spontaneous activation.

The field-effect transistor FET PSMN4R3-30BL (Nexperia, China) controlled by a PWM signal coming from MCU is used as the control element VT1 as described in [6]. This transistor is selected with allowance for power dissipation and the required output characteristics[8]; the control voltage produced by the divider R9, R10 is only 4.5 V.

The transistor output characteristic (Fig. 4) shows the transistor to be capable of commutating direct current up to 100 A at the control voltage of 4.5 V.

Although this value is much higher than necessary for steady-state operation, very high currents occur between C13, C15 and C21 when the output filters are powered due to the capacitors C13 and C15 having a rated capacity of 4700 μF. The equivalent series resistance of these capacitors is 55 mΩ; when unlocking the transistor gate[9], the peak current may be written as follows:

$$I_{peak} = \frac{U_{out}}{R_{ESR}} = \frac{23.75}{0.055} = 431.8\ \text{A}, \quad (2)$$

where U_{out} is the source voltage; R_{ESR} is the equivalent series resistance of the capacitor.

Here, the subsequent capacitive filter elements are not accounted for: the current is limited by the step-up

[6] High performance, low power AVR® 8-bit microcontroller, ATmega48/V/88/V/168/V, DS40002074A. Microchip Technology; 2018. 390 p. https://www.microchip.com/content/dam/mchp/documents/OTH/ProductDocuments/DataSheets/ATmega48_88_168_megaAVR-Data-Sheet-40002074.pdf. Accessed August 29, 2022.

[7] Switching current boost / buck-boost / inverting DC/DC converter, XL6009. Xinlong Semiconductor Technology; 2017. 8 p.

[8] N-channel MOSFET in D2PAK, PSMN4R3-30BL. Nexperia B.V.; 2017. 15 p.

[9] Matvienko V.A. *Fundamentals of electric circuit theory*: Textbook for universities; Yekaterinburg: UMTs UPI; 2016. 162 p. (in Russ.).

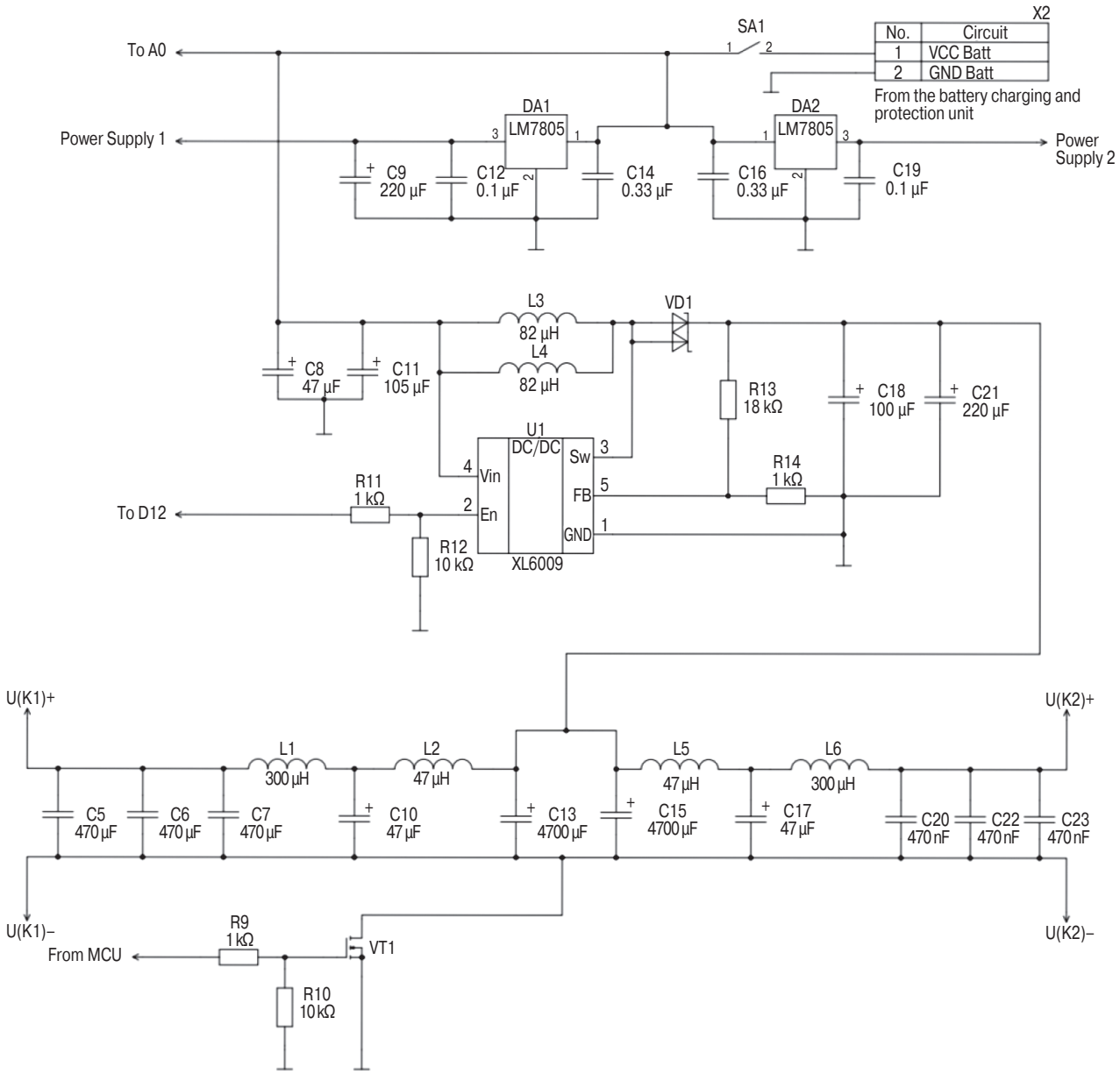

Fig. 3. Power supply circuit diagram of the monitoring and control unit. Here and in the following circuits, the designations of elements correspond to GOST 2.710-81[10]

voltage regulator U1, but not until its output capacities are discharged. Since the maximum peak current of the selected transistor is 465 A, the performance is not affected.

Each output filter is the LC ladder filter, as described in [7]. These are used for additional smoothing of pulsations after the boost converter.[11]

Both 5V linear voltage regulators are made on LM7805 chips (Inchange Semiconductor Company, China). The C14 and C16 capacitors filter input pulsations, while the C9, C12, and C19 capacitors filter the output ones.

The commutating elements K1–K3 (Fig. 5) are implemented on HK19F-DC5V-SHG relay (Ever-way Industry Co, China). The rated commutation current is 2 A at DC voltage 30 V[12]. The relay is controlled from MCU through optocouplers DA3–DA5. Resistors R15–R17 limit the current through the optocoupler and the LED used for indicating the state of elements K1–K3. This implementation allows for galvanic isolation of the MCU pin and the relay to protect MCU from line voltage as described in [8].

[10] GOST 2.710-81. Unified system for design documentation. Alpha-numerical designations in electrical diagrams. Moscow: Izdatel'stvo standartov; 1985 (in Russ.).

[11] Output noise filtering for DC/DC power modules. https://www.ti.com/lit/an/snva871/snva871.pdf. Accessed August 29, 2022.

[12] Subminiature DIP Relay, HK19F. Ever-Way Industry Company Limited; 2011. 3 p.

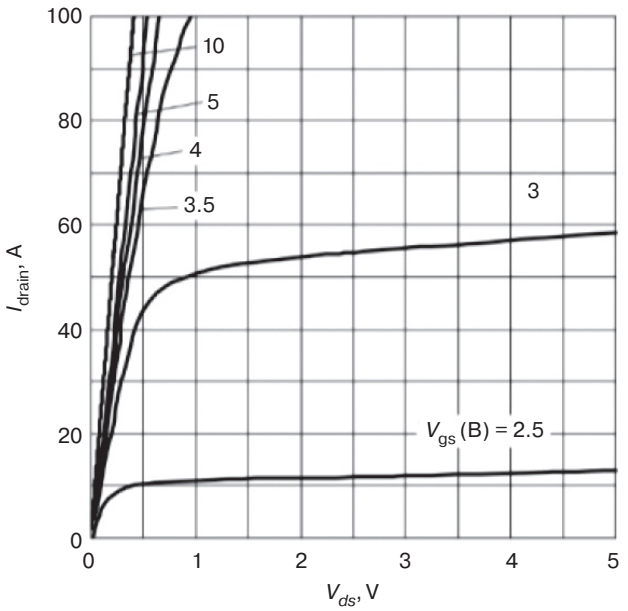

Fig. 4. Output characteristic of the PSMN4R3-30BL transistor. Dependence of the drain current I_{drain} on the drain–source voltage V_{ds} at fixed gate–source voltages V_{gs}

All the sensors used are connected via the I²C bus (Fig. 6). The INA219 chip (Texas Instruments, USA), which determines the current and voltage with an accuracy of ±0.2%[13], is used as the current, voltage, and power sensor. The SHT2 chip (Sensirion AG, Switzerland) is used as a temperature and humidity sensor; it has an accuracy of relative humidity ±2% and temperature ±0.3 °C.[14]

The LEDs HL1–HL4 displaying the remaining battery percentage along with the system operating mode are used as indicators; SB1 is the MCU reset button. The SB2 and SB3 clock buttons used for the forced shutdown of UPS output channels are connected to the MCU analog input DD1 through the resistive divider.

3. BATTERY CHARGING AND PROTECTION UNIT

The structural diagram of the battery charging and protection unit is shown in Fig. 7.

In the designed system, the load for this unit is produced by the control and monitoring unit. The circuit diagram of the battery-charging and protection unit is shown in Fig. 8, 10, and 11. The standalone pulse charge controller for the Li+ battery is implemented on a MAX1737 chip (Maxim integrated, USA) (Fig. 8). This controls the input current from the source, the output charging current, and the battery voltage. The allowable charging voltages range between 4.0 V per cell and 4.4 V per cell.

[13] Ugryumov E.P. *Digital circuitry*: Textbook for universities. 2nd ed.; BHV-Petersburg; 2007. 800 p. (in Russ.).

[14] Humidity and Temperature Sensor IC, SHT21. SENSIRION. CMOSens®; 2014. 15 p.

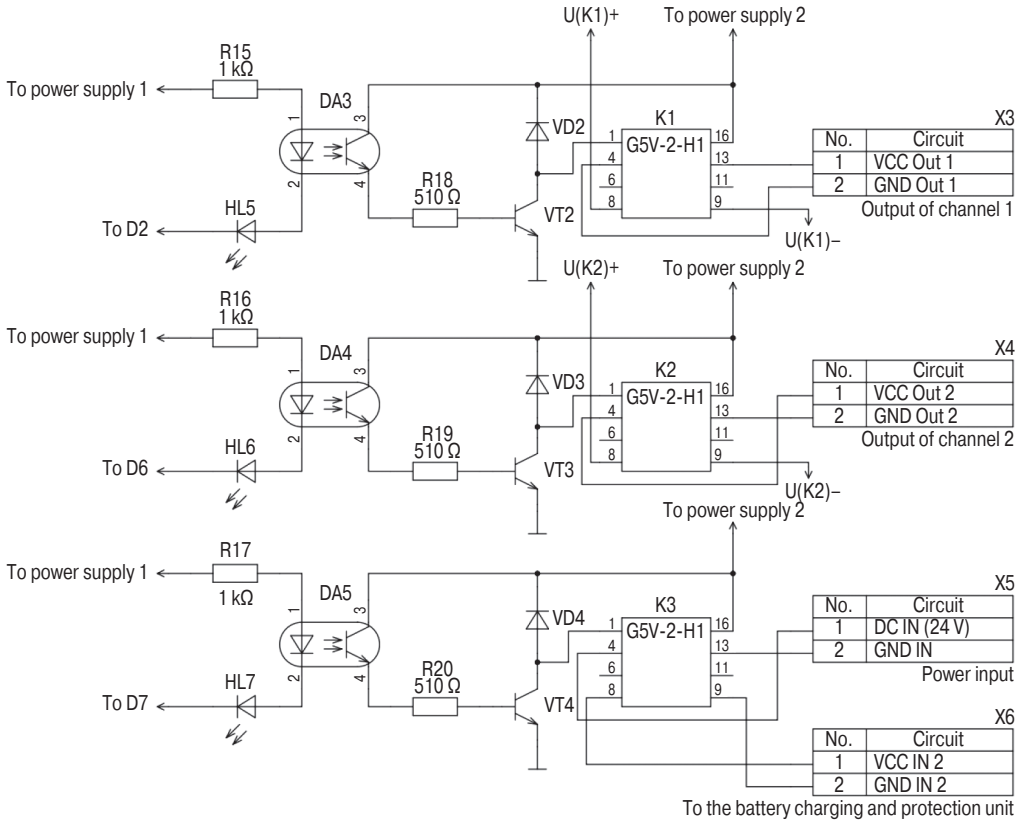

Fig. 5. Circuit diagram of commutating elements for the monitoring and control unit

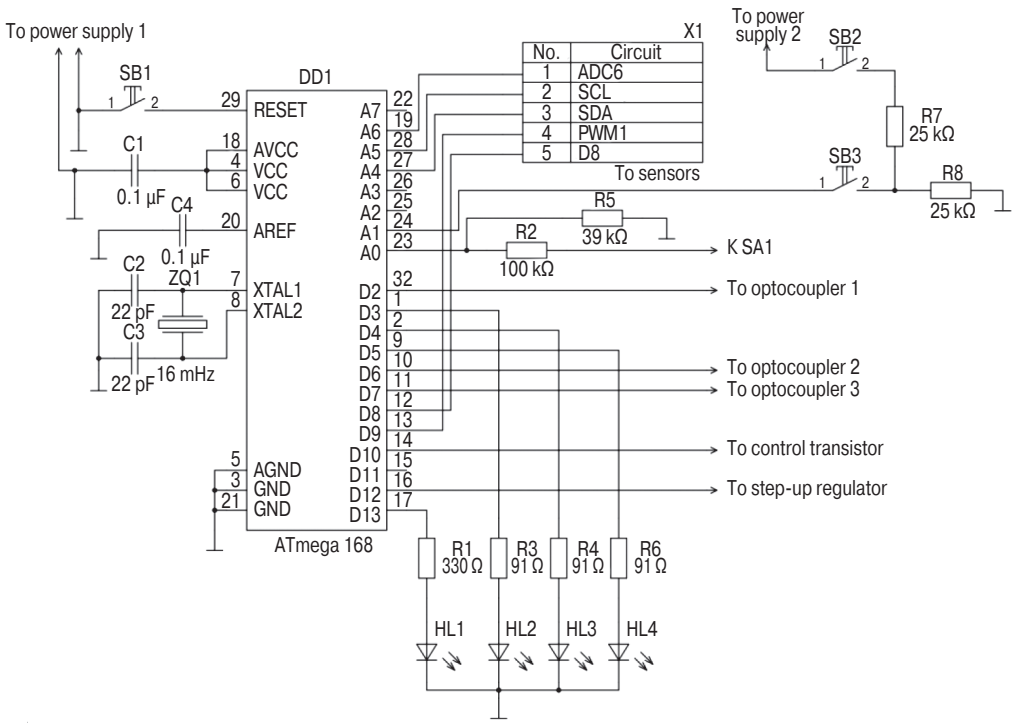

Fig. 6. Circuit diagram of the monitoring and control unit MCU

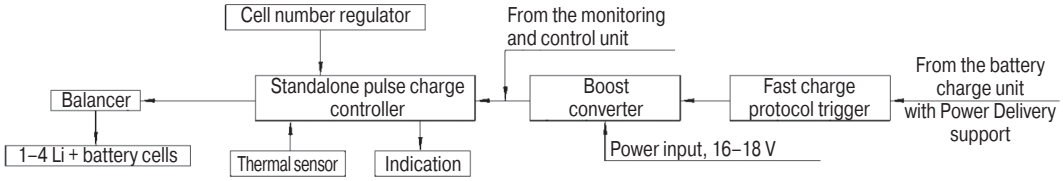

Fig. 7. Structural diagram of the battery charging and protection unit

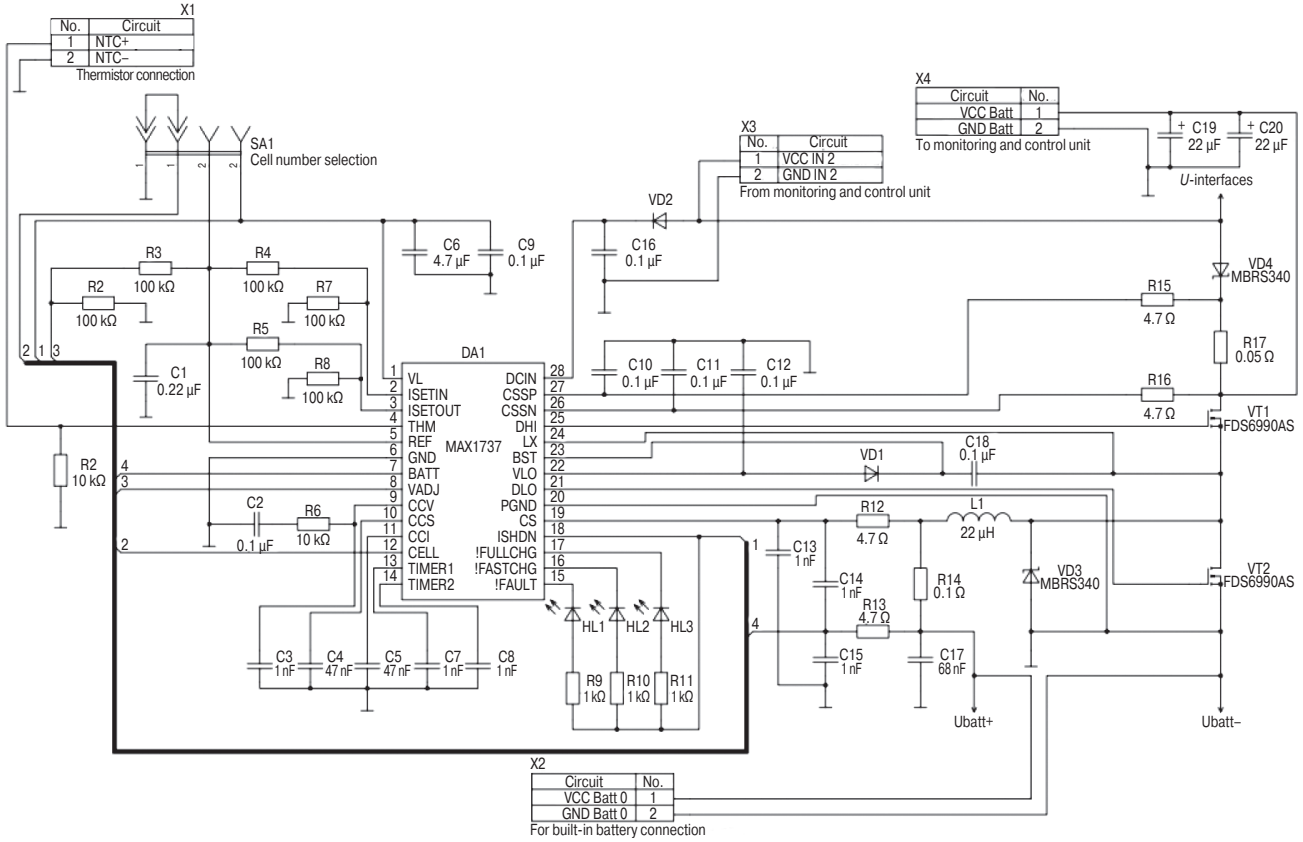

Fig. 8. Circuit diagram of the battery charging and protection unit controller

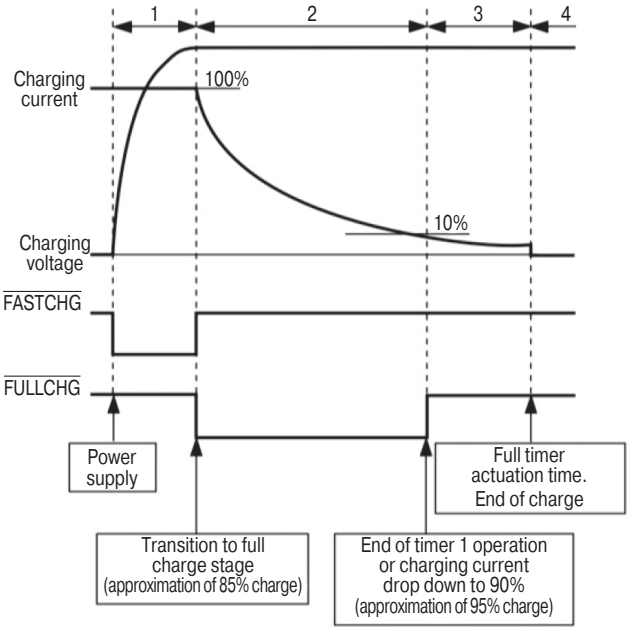

Fig. 9. Diagrams of voltage and current for charging profile

The external thermistor is connected via connector X1. The 10 kΩ resistor R1 is installed in the absence of a need for temperature monitoring. When the voltage of the built-in battery drops below the minimum threshold value U_{min} (3), the deep discharge protection system is activated; the load is switched off by transistors VT1 and VT2.

$$U_{min} = 2.5N \text{ V}, \quad (3)$$

where N is the number of connected cells.

The Li+ batteries are charged according to the specific charging profile, which is distinguished from those used with classic lead acid batteries. This is necessary for increasing the lifetime of the batteries as detailed in [9] and recommended for charging by many Li+ battery manufacturers. The diagram of the charging voltage and current as well as voltage diagrams of inverting pins for the fast charge (FASTCHG) and full charge (FULLCHG) stages are shown in Fig. 9.

The full charge cycle may be divided into 4 main stages:

1) fast charge stage—including non-linear changes in battery voltage while the current remains constant;
2) full charge stage—battery voltage reaches the predetermined value to remain constant, while the current decreases;
3) fill stage—initial current is decreased by 90% while the current change becomes almost linear;
4) completion stage—charging current becomes zero.

The maximum duration of each cycle is set by the charge controller's internal timers. The nominal value of capacitor C8 sets the running time of timer 2 responsible for the fast charge stage, amounting to 90 min at 1 nF. Should the controller fail in transiting to the next stage of the charge cycle within the time set by timer 2, the chip disables further battery charging and turns the error indicator on.

The nominal value of capacitor C7 sets the running time of timer 1 responsible for the full charge and fill stages, as well as for the pre-preparation time. At 1 nF, the full charge stage time is 90 min, while the fill stage time is 45 min. The pre-preparation includes checking the cell voltage for the minimum threshold value as well as checking the temperature. The checking time is 7.5 min. Should indicated values exceed the operating range, the controller turns an error message on and the charge cycle does not begin.

The LEDs HL1–HL3 are connected via current limiting resistors R9–R11 to inverting pins of the charge controller state indicator FAULT, FASTCHG, and FULLCHG.

The elements VT1, VT2, C17, L1, and VD3 form the DC voltage step-down converter. The transistor gates are controlled by chip DA1 (Maxim integrated, USA). This chip generates a PWM signal with variable fill factor depending on the input and the battery charging voltages and a frequency of 300 kHz. The claimed conversion efficiency ranges from 85% to 90%[15]. Although the output voltage ranges from 6 to 28 V, the input voltage should be higher than the minimum supply voltage of the charge controller:

$$U_{min\ chg} = U_{min} + 1.6 \text{ V}. \quad (4)$$

The voltage drop across resistor R17 sets the input current of the charge controller I_{in} as calculated by the following formula:

$$I_{in} = \frac{0.1}{R_{17}} \cdot \frac{U_{ISETIN}}{U_{REF}} = 1 \text{ A}, \quad (5)$$

where U_{ISETIN} is the voltage on pin 2 (SETIN) DA1 set by the voltage divider formed by resistors R4 and R7 with reference voltage at the input U_{REF} = 4.166–4.242 V.

The voltage drop across resistor R14, which regulates the battery charging current I_{chg}, is calculated by the following formula:

$$I_{chg} = \frac{0.2}{R_{14}} \cdot \frac{U_{ISETOUT}}{U_{REF}} = 1 \text{ A}, \quad (6)$$

where $U_{ISETOUT}$ is the voltage on pin I_{SETOUT} set by the voltage divider formed by resistors R5 and R8 with reference voltage at the input U_{REF}.

[15] Stand-alone switch-mode lithium-ion battery-charger controller, MAX1737, Data Sheet 19-1626. Maxim Integrated; 2017. 19 p.

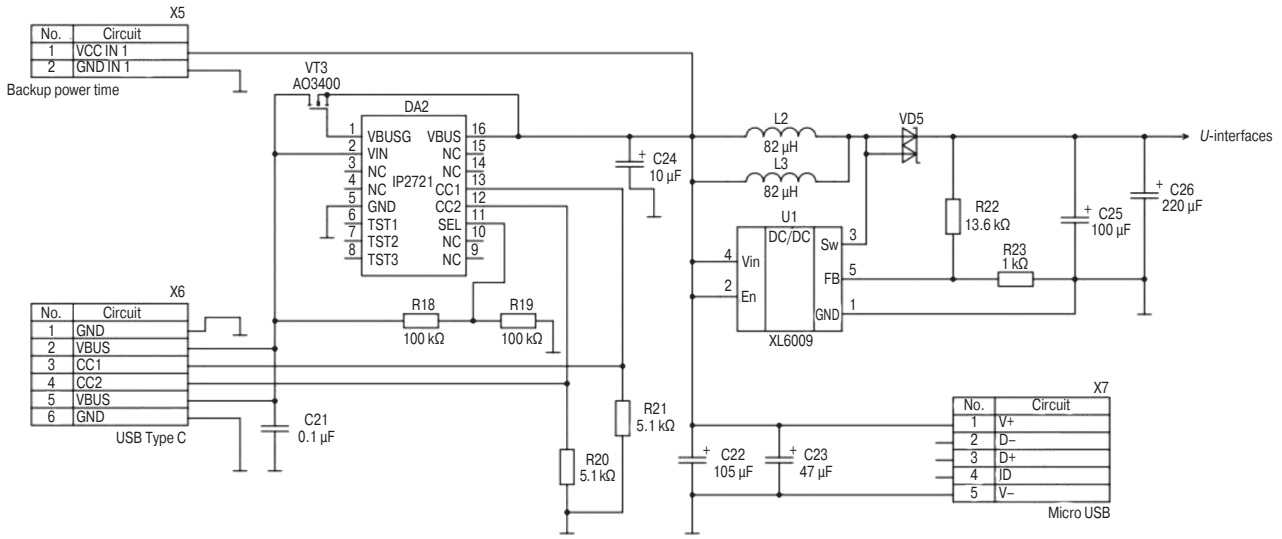

Fig. 10. Circuit diagram of the boost converter of the battery charging and protection unit

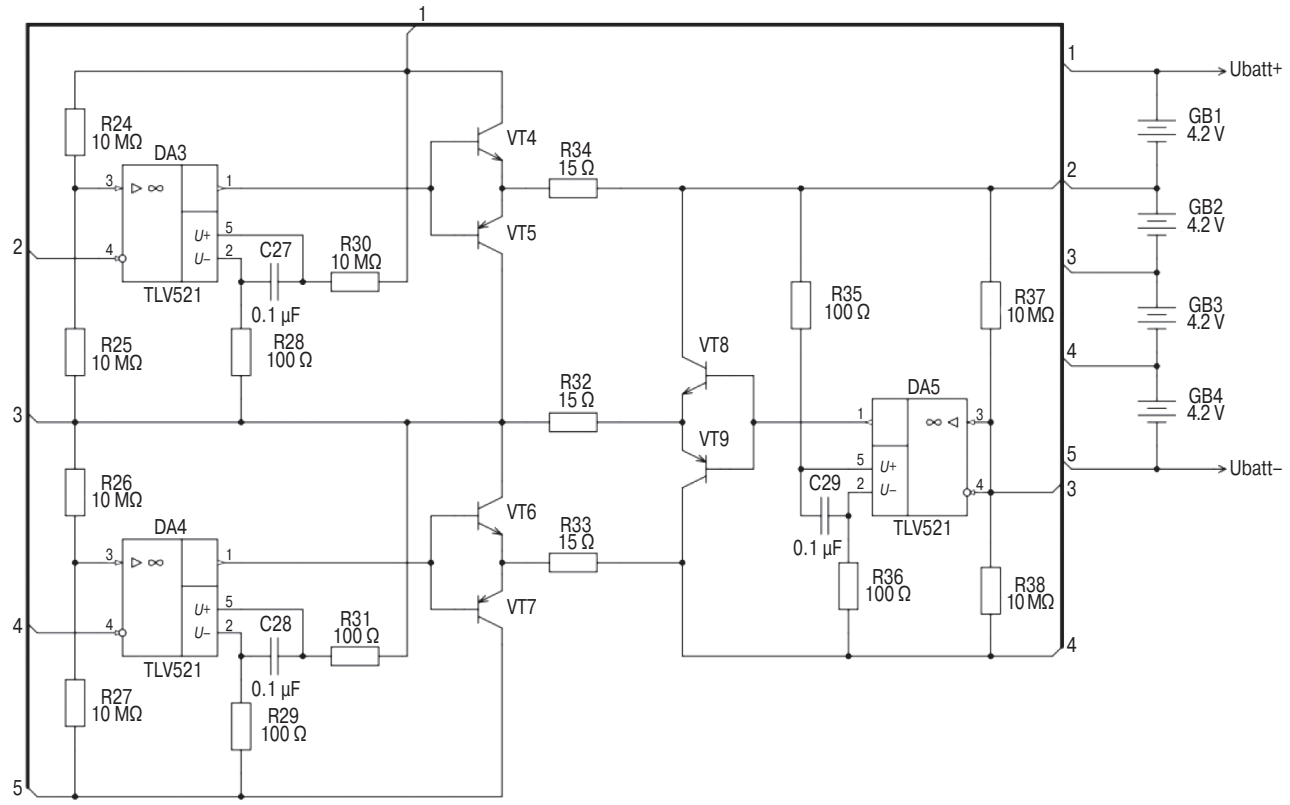

Fig. 11. Circuit diagram for the balancing module of the battery charging and protection unit

The boost converter in the battery charging and protection unit (Fig. 10) is used for generating the supply voltage of the charge controller. As a result, the input charging voltage range of the built-in battery is significantly extended, ranging from 5 to 28 V regardless of how many cells are connected due to the formation of a step-up/down converter.

The support of the Power Delivery fast charging protocol implemented in many modern consumer battery chargers is provided by the protocol trigger implemented on the IP2721 chip (Injoinic Technology Corp., China). Pin SEL sets one of the standard output voltages of the connected charger using data exchange protocol. When pin SEL is connected via resistor R18 to the power supply, the voltage at the battery charger unit is set to 12 V; when it is connected via resistor R19 to "ground", the voltage is set to 5 V.[16]

[16] TYPEC/PD2.0/PD3.0 Physical Layer IC for USB TYPEC input interfaces, IP2721. Injoinc Corp.; 2017. 7 p.

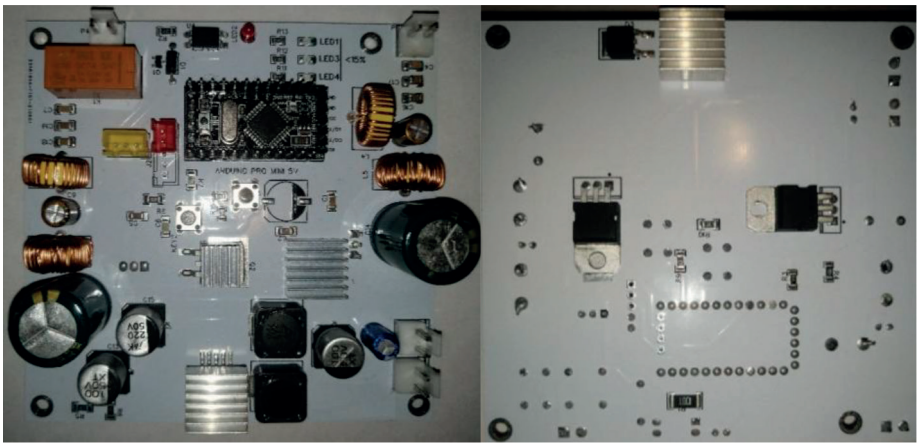

Fig. 12. Prototype for the monitoring and control unit: top and bottom views

Fig. 13. Prototype for the battery charging and protection unit: top and bottom views

The built-in cells are balanced by the balancing module using operational amplifiers DA3, DA4, and DA5 (Fig. 11). Each of these controls a pair of transistors by comparing the sum of voltages on two battery cells with voltage between two cells connected in series making allowance for the voltage[17] divider formed by a pair of resistors R24–R25 for DA3, R26–R27 for DA4 and R37–R38 for DA5. The built-in battery is formed by the cells of Li+ batteries GB1–GB4 connected in series. Operational amplifiers TLV521 (Texas Instruments, USA) are selected due to low power consumption[18], which increases energy efficiency.

The prototype design for the monitoring and control unit is shown in Fig. 12.

The prototype design for the battery charging and protection unit is shown in Fig. 13.

[17] Keep the balance – balancing of supercapacitors, ANP090. https://www.we-online.com/catalog/media/o671684v410%20ANP090a%20EN.pdf. Accessed August 29, 2022.

[18] NanoPower, 350nA, RRIO, CMOS Input, operational amplifier, TLV521, Data Sheet SNOSD26. Texas Instruments; 2016. 27 p.

4. RESEARCH FINDINGS ON CHARACTERISTICS OF THE DEVELOPED SYSTEM

For evaluating the output power of two channels, each channel is connected to a controlled electronic load. The constant power operating mode is set to 20 W per channel. The total power delivered by the system to the electronic load is about 40 W in this operating mode. Time diagrams for current, voltage, and power are drawn using the measuring tools built into the electronic load units.

Time diagrams for current, voltage, and power of the first channel are shown in Figs. 14 and 15.

Figure 14 shows that the change in the output voltage level during operation is 0.2 V. The actual output voltage level is 22.6 V differing from the calculated value U_{out}. This is due to the voltage drop across the output filters and the parameter spread of resistors R13, R14. The output current ripple is due to the operating principle of the controlled electronic load.

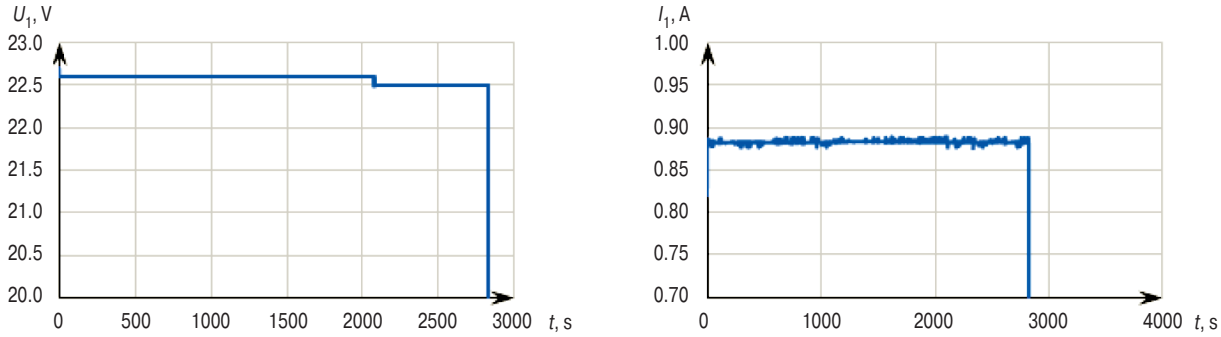

Fig. 14. Time diagrams for current and voltage of the first channel

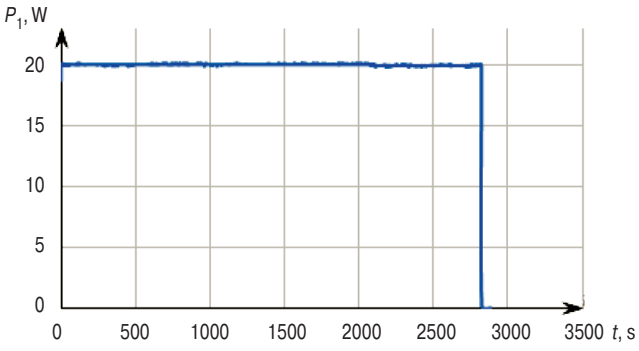

Fig. 15. Time diagram of the first channel power

Time diagrams of the second channel almost coincide with those of the first one making allowance for the insignificant parameter spread of the output filters. Time diagrams for the total current and power of two channels are shown in Fig. 16.

It may be seen from Figs. 14–16 that a sudden drop in the output voltage and power level occurs at t = 2800 s. This is due to automation; the voltage of built-in batteries drops below the critical value, they are completely discharged, and the charge controller disconnects them from the monitoring and control unit.

As can be seen from Fig. 16, the total output power is about 40 W, while the system operating time with such load is at least 45 min.

CONCLUSIONS

A prototype of an uninterruptible power system with the ability to change output voltage for required tasks has been created. Each unit has been tested separately along with their interaction.

The system generates stable output voltage of 22.6 V with a power of 20 W in each channel. The monitoring and control unit correctly displays the remaining percentage of the built-in battery charge in increments of 25% and enables shutdown of consumers when the built-in battery voltage falls below a specified threshold, thus duplicating the protection function of the battery charging and protection unit.

The battery charging and protection unit provides stable power supply to the monitoring and control unit for at least 45 min, successfully activating the fast-charging protocol when connected to the battery charger and protecting the built-in batteries from "overcharging."

It is intended to improve the developed system in future as follows:

- modification of output filters for reducing output voltage ripple;
- improvement of DC-DC converter input filters for reducing noise level;[19]

[19] Design and application considerations of input filter to reduce conducted emissions caused by DC/DC converter, No. 62AN101E Rev.003. ROHM Co., Ltd.; 2020. 7 p.

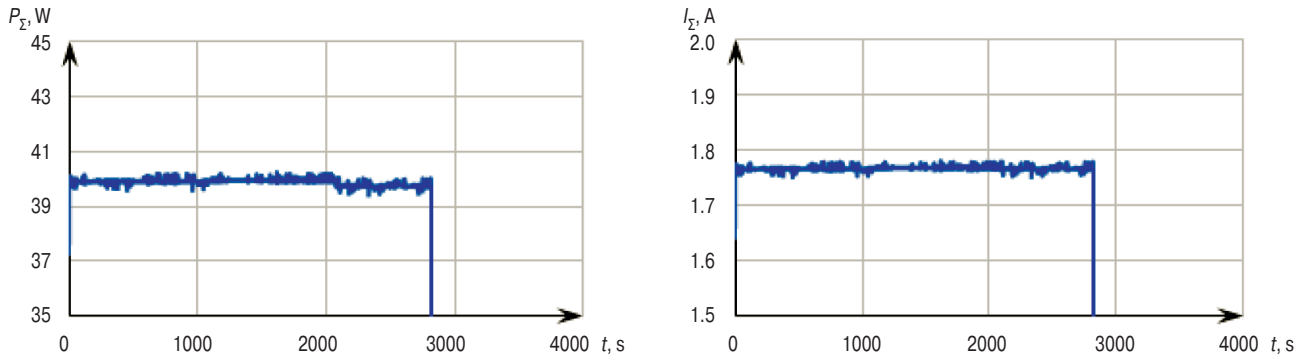

Fig. 16. Time diagrams for the total current and power of two channels

- replacement of transistor group in the balancing module for increasing maximum allowable balancing currents or using the balancing module for the same purpose;[20]
- increasing the output power and developing the inverter for providing the standard 220 V network voltage;
- implementing the control of the charge controller from MCU.

[20] Passive balancing allows all cells to appear to have the same capacity. https://softei.com/passive-balancing-allows-all-cells-to-appear-to-have-the-same-capacity. Accessed August 29, 2022.

Authors' contribution
All authors equally contributed to the research work.

REFERENCES

1. Lukutin B.V., Muravlev I.O., Plotnikov I.A. *Sistemy elektrosnabzheniya s vetrovymi i solnechnymi elektrostantsiyami*: uchebnoe posobie (*Power supply systems with wind and solar power plants*: textbook). Tomsk: Publishing House of Tomsk Polytechnic University; 2015. 128 p. (in Russ.).
2. Datsenko V.A., Sivkov A.A., Gerasimov D.Yu. *Montazh, remont i ekspluatatsiya elektricheskikh raspredelitel'nykh setei v sistemakh elektrosnabzheniya promyshlennykh predpriyatii*: uchebnoe posobie (*Installation, repair and operation of electrical distribution networks in power supply systems of industrial enterprises*: textbook). Tomsk: Publishing House of Tomsk Polytechnic University; 2007. 132 p. (in Russ.).
3. Traister J.E., Kennedy T. *Low voltage wiring: Security/Fire alarm systems*. NY: The McGraw-Hill Companies; 2002. 408 p.
4. Bityukov V.K., Lukht M.A., Mikhnevich N.G., Petrov V.A. Mother board of trainer with virtual front panel for study of linear voltage regulator characteristics. *Russ. Technol. J.* 2017;5(4):22–31 (in Russ.). https://doi.org/10.32362/2500-316X-2017-5-4-22-31
5. Revich Yu.V. *Programmirovanie mikrokontrollerov AVR: ot Arduino k assembleru* (*Programming of AVR microcontrollers: from Arduino to Assembler*). St. Petersburg: BHV-Petersburg; 2020. 448 p. (in Russ.). ISBN 978-5-9775-4076-6
6. Bityukov V.K., Simachkov D.S., Babenko V.P. *Istochniki vtorichnogo elektropitaniya* (*Secondary power sources*). Moscow; Vologda: Infra-Inzheneriya; 2020. 376 p. (in Russ.). ISBN 978-5-9729-0471-6
7. Milenina S.A., Milenin N.K. *Elektrotekhnika, elektronika i skhemotekhnika*: uchebnik i praktikum dlya vuzov (*Electrical engineering, electronics and circuit engineering*: textbook and workshop for universities). Moscow: Yurait; 2021. 406 p. (in Russ.). ISBN 978-5-534-04525-3
8. Gololobov V.N. *Skhemotekhnika s programmoi Multisim dlya lyuboznatel'nykh* (*CIRCUIT DESIGN with the Multisim program for the curious*). St. Petersburg: Nauka i tekhnika; 2019. 272 p. (in Russ.). ISBN 978-5-94387-880-0
9. Methekar P.N., et al. Optimum charging profile for lithium-ion batteries to maximize energy storage and utilization. *ECS Trans*. 2010;25(35):139–146. https://doi.org/10.1149/1.3414012

СПИСОК ЛИТЕРАТУРЫ

1. Лукутин Б.В., Муравлев И.О., Плотников И.А. *Системы электроснабжения с ветровыми и солнечными электростанциями:* учебное пособие. Томск: Изд-во Томского политехнического университета; 2015. 128 с.
2. Даценко В.А., Сивков А.А., Герасимов Д.Ю. *Монтаж, ремонт и эксплуатация электрических распределительных сетей в системах электроснабжения промышленных предприятий:* учебное пособие. Томск: Изд-во Томского политехнического университета; 2007. 132 с.
3. Traister J.E., Kennedy T. *Low voltage wiring: Security/Fire alarm systems*. NY: The McGraw-Hill Companies; 2002. 408 p.
4. Битюков В.К., Лухт М.А., Михневич Н.Г., Петров В.А. Системная плата учебного лабораторного стенда с виртуальной передней панелью для исследований характеристик линейных стабилизаторов. *Российский технологический журнал*. 2017;5(4):22–31. https://doi.org/10.32362/2500-316X-2017-5-4-22-31
5. Ревич Ю.В. *Программирование микроконтроллеров AVR: от Arduino к ассемблеру*. СПб.: БХВ-Петербург; 2020. 448 с. ISBN 978-5-9775-4076-6
6. Битюков В.К., Симачков Д.С., Бабенко В.П. *Источники вторичного электропитания*. Москва; Вологда: Инфра-Инженерия; 2020. 376 с. ISBN 978-5-9729-0471-6
7. Миленина С.А., Миленин Н.К. *Электротехника, электроника и схемотехника*: учебник и практикум для вузов. М.: Юрайт; 2021. 406 с. ISBN 978-5-534-04525-3
8. Гололобов В.Н. *Схемотехника с программой Multisim для любознательных*. СПб.: Наука и техника; 2019. 272 с. ISBN 978-5-94387-880-0
9. Methekar P.N., et al. Optimum charging profile for lithium-ion batteries to maximize energy storage and utilization. *ECS Trans*. 2010;25(35):139–146. https://doi.org/10.1149/1.3414012

About the authors

Igor M. Sharov, Student, Department of Radio Electronic Systems and Complexes, Institute of Radio Electronics and Informatics, MIREA – Russian Technological University (78, Vernadskogo pr., Moscow, 119454 Russia). E-mail: ctosworld@gmail.com. https://orcid.org/0000-0002-3391-3266

Oleg A. Demin, Student, Department of Radio Electronic Systems and Complexes, Institute of Radio Electronics and Informatics, MIREA – Russian Technological University (78, Vernadskogo pr., Moscow, 119454 Russia). E-mail: coin12@mail.ru. https://orcid.org/0000-0002-9864-5338

Alexander A. Sudakov, Assistant, Department of Radio Electronic Systems and Complexes, Institute of Radio Electronics and Informatics, MIREA – Russian Technological University (78, Vernadskogo pr., Moscow, 119454 Russia). E-mail: sudakov@mirea.ru. RSCI SPIN-code 4225-2792, https://orcid.org/0000-0001-6958-8111

Alexey D. Yarlykov, Assistant, Department of Radio Wave Processes and Technologies, Institute of Radio Electronics and Informatics, MIREA – Russian Technological University (78, Vernadskogo pr., Moscow, 119454 Russia). E-mail: yarlykov@mirea.ru. Scopus Author ID 57290652000, RSCI SPIN-code 3450-1587, https://orcid.org/0000-0002-7232-8588

Об авторах

Шаров Игорь Михайлович, студент, кафедра радиоэлектронных систем и комплексов Института радиоэлектроники и информатики ФГБОУ ВО «МИРЭА – Российский технологический университет» (119454, Россия, Москва, пр-т Вернадского, д. 78). E-mail: ctosworld@gmail.com. https://orcid.org/0000-0002-3391-3266

Демин Олег Александрович, студент, кафедра радиоэлектронных систем и комплексов Института радиоэлектроники и информатики ФГБОУ ВО «МИРЭА – Российский технологический университет» (119454, Россия, Москва, пр-т Вернадского, д. 78). E-mail: coin12@mail.ru. https://orcid.org/0000-0002-9864-5338

Судаков Александр Анатольевич, ассистент, кафедра радиоэлектронных систем и комплексов Института радиоэлектроники и информатики ФГБОУ ВО «МИРЭА – Российский технологический университет» (119454, Россия, Москва, пр-т Вернадского, д. 78). E-mail: sudakov@mirea.ru. SPIN-код РИНЦ 4225-2792, https://orcid.org/0000-0001-6958-8111

Ярлыков Алексей Дмитриевич, ассистент, кафедра радиоволновых процессов и технологий Института радиоэлектроники и информатики ФГБОУ ВО «МИРЭА – Российский технологический университет» (119454, Россия, Москва, пр-т Вернадского, д. 78). E-mail: yarlykov@mirea.ru. Scopus Author ID 57290652000, SPIN-код РИНЦ 3450-1587, https://orcid.org/0000-0002-7232-8588

Translated from Russian into English by Kirill V. Nazarov
Edited for English language and spelling by Thomas A. Beavitt